

Supplemental Material

Supplemental Methods

Tissue Acquisition

Fresh human adipose tissues (pericardial, visceral and subcutaneous, $n=24$, 68 and 28, respectively.) were obtained as discarded surgical specimens from a total of 120 patients undergoing abdominal surgeries or cardiopulmonary by-pass procedures, and unused whole hearts ($n=14$) from Donor Network. After surgical removal, specimens were placed in ice-cold HEPES buffer or in a cardioplegic buffer solution (for heart tissue) and immediately transferred to the laboratory for isolated vessel studies. De-identified patient demographic data were collected using the Generic Clinical Research Database (GCRD) at the Medical College of Wisconsin. All protocols were approved by the Institutional Review Board of the Medical College of Wisconsin and Froedtert Hospital. Patient demographic information is summarized in Online Table I.

Cell Culture and Transfection

HEK-293 cells were provided by Dr. David Wilcox (Medical College of Wisconsin) and grown in DMEM supplemented with 10% FBS, 100 U/mL penicillin G, and 100 μ g/mL streptomycin at 37 °C and 5% CO₂. HEK-293 cells were used for the present study between passages 6 and 10.

The full-length human K_vα1.5 cDNA clone was obtained from Origene and subcloned into pCMV6 mammalian expression vectors as a fusion protein with the COOH-terminus of K_vα1.5 tagged with a FLAG tag. The nucleic sequence of K_vα1.5-FLAG constructs was verified by direct DNA sequencing. K_vα1.5-FLAG coding plasmids were isolated by an endotoxin-free plasmid kit (Qiagen), and transiently transfected into HEK-293 cells using the lipid-mediated lipofectamine 2000 kit (Invitrogen) according to the manufacturer's protocols. In brief, cells were plated in 60-mm petri dishes 16-24 h before transfection. Cells were transfected with 2 μ g plasmid DNA/60-mm dish and used 24-48 h after transfection.

Enzymatic Isolation of Vascular Cells

Smooth muscle cells (SMCs) were enzymatically dissociated from arteries as previously described.^{1,2} In brief, artery segments were cut into small rings and incubated for 10 min at room temperature in a low-Ca²⁺ dissociation solution consisting of (in mmol/L) 140 NaCl, 5.0 KCl, 0.05 CaCl₂, 1.0 MgSO₄, 10 glucose, and 10 HEPES, with 0.1% BSA (pH 7.4). The solution was carefully removed and vessel segments were incubated with papain (1.0 mg/mL) and dithiothreitol (0.5 mg/mL) in dissociation solution for 15 min at 37°C, followed by incubation with collagenase (Sigma blend H; 1.0 mg/mL), trypsin inhibitor (1 mg/mL), and elastase (0.5 mg/mL) in dissociation solution for 15-30 min at 37°C. All enzymes and chemicals were purchased from Sigma. Artery segments were then gently triturated to release smooth muscle cells. The dissociated cells were washed twice in dissociation solution by centrifugation at 250 × g for 5 min. Cells were stored on ice or at 4°C and used the same day for immunocytochemistry as described below.

Videomicroscopy

Small arterioles (internal diameter 100-250 μ m) from fresh human adipose tissue were carefully dissected. Vessels were cannulated with two glass micropipettes for continuous measurements of diameter with a video system as previously described.¹ Vessels were pressurized to an intramural pressure of 60 mmHg under no-flow conditions and equilibrated for 1 hour at 37°C in modified Krebs-physiological saline solution (in mmol/L; NaCl 123, KCl 4.7, MgSO₄ 1.2, CaCl₂ 2.5, NaHCO₃ 19, KH₂PO₄ 1.2, EDTA 0.026, and glucose 11) continuously gassed with a mixture of 21% O₂, 5%, CO₂ and 74% N₂ to maintain pH 7.4.

To study vasodilator response, arterioles were precontracted with endothelin-1 (0.1-0.5 nmol/L) to approximately 30% to 50% of the baseline internal diameter. After the contraction

reached steady state, relaxation responses to cumulative concentrations of H₂O₂ (1-100 μmol/L) were determined in the absence and presence of 20-30 minutes preincubation with one of the following modulators alone or in combination: N^G-nitro-L-arginine methyl ester (L-NAME, 100 μmol/L), a nitric oxide synthase (NOS) inhibitor; indomethacin (10 μmol/L), a cyclooxygenase inhibitor; 4-aminopyridine (4-AP, 10 mmol/L), a non-selective voltage-dependent K⁺-channel blocker; paxilline (100 nmol/L), a specific and cell-permeable BK_{Ca} channel blocker; iberiotoxin (100 nmol/L), a specific but not cell-permeable BK_{Ca} channel blocker; diphenyl phosphine oxide-1 (DPO-1, 1 μmol/L), selective a K_vα1.5 channel blocker; 5-(4-phenylbutoxy)psoralen (Psora-4, 30 nmol/L), a selective K_vα1.3/α1.5 channel blocker; phenoxyalkoxypsoralen-1 (PAP-1, 10 nmol/L), a selective K_vα1.3 channel blocker; 1-benzyl-4-pentylimino-1,4-dihydroquinoline (CP-339818, 3 μmol/L), a selective K_vα1.3/α1.4 channel blocker; Stromatoxin (100 nmol/L), a selective K_vα2.1, K_vα2.1/α9.3 blocker; DL-dithiothreitol (DTT, 3 mmol/L), a membrane-permeant thiol-specific reducing agent; Tris(2-carboxyethyl)phosphine (TCEP, 5 mmol/L), a membrane-impermeable thiol-reducing agent; and catalase (1000 U/mL), a H₂O₂ metabolizing enzyme. To examine the role of smooth muscle hyperpolarization in H₂O₂-induced dilation, vessels were constricted with a High-K⁺ (60 mmol/L) Krebs-PSS.

In some vessels, the endothelium was removed by perfusing 3-5 mL of air through the lumen. The endothelium was considered intact if acetylcholine (10 μmol/L) caused >80% relaxation of endothelin-1-constricted vessels and effectively denuded if acetylcholine induced <10% relaxation. At the end of each experiment, papaverine (100 μmol/L), an endothelium independent vasodilator, was added to the vessel bath to determine the maximal internal diameter for normalization of dilator responses. Unless otherwise stated, experiments were performed on endothelium-intact arterioles and in the presence of L-NAME and Indomethacin.

RNA extraction and reverse transcription-polymerase chain reaction

Human adipose arteries and arterioles (200-500 μm) freshly dissected were snap-frozen in liquid nitrogen and store at -80°C until use. In some vessels, the endothelium was removed by gentle scraping of the lumen of vessels. Total RNA was extracted with RNeasy Fibrous Tissue Mini Kit (Qiagen) and cDNA synthesized using SuperScript III reverse transcriptase (Invitrogen), according to the manufacturer's instructions. Unless otherwise stated, a total of 2-5 ng input RNA (cDNA) was amplified in a Peltier thermal cycler (MJ Research, model PTC-200) using Platinum PCR Supermix (Invitrogen) and a 40-45-cycle touch-down protocol.¹ The gene-specific primers were synthesized by IDT Integrated DNA Technologies, Inc. (Coralville, Iowa), with detailed sequence information in Supplemental Online Table II. Two negative controls, without reverse transcription (RT-) and without template (H₂O), were amplified in parallel by using K_vα9.3 primers. Human brain total RNA samples from a normal donor (Agilent Technologies, Santa Clara, CA) were included as a positive control. Human brain tissue is known to express all 11 subunits of K_v channels and BK_{Ca} channel examined in this study.³

Quantitative PCR was performed using CFX96 C1000 Thermal Cycler (BioRad). The reactions were conducted in a 20 μL volume containing 10 μL 2x All-in-One SYBR Green qPCR mix (GeneCopoeia) or SsoAdvanced Universal SYBR Green Supermix (for siRNA qPCR, BioRad), 2 μL (each for forward and reverse) of K_vα1.5-specific primers, nuclease-free water and 2 μL of pooled or individual (for siRNA qPCR) sample cDNA (2 ng). Pooled sample cDNA was prepared by extracting mRNA and synthesizing cDNA from each tissue sample individually. An equal amount of cDNA from each sample was then added to create pooled samples for each non-CAD and CAD group. Cycle threshold (Ct) values of products were determined using Bio-Rad CFX Manager 3.1 software (BioRad). Relative K_vα1.5 gene expression was normalized to average of β-actin and ATP5o genes.⁴ For primer sequences refer to Online Table III. The thermal profile employed 1 cycle of initial denaturation at 95°C for 5 min, 40 cycles of denaturation at 95°C for 10 sec, annealing at 60°C for 30 sec and extension at 72°C for 15 sec. Melting curve analysis was performed immediately after the 40th cycle at 72 to 95°C with 0.5 degree increments for 5

sec. Comparative Ct Method was used to calculate relative expression of $K_v\alpha 1.5$ subunit, where CAD was normalized to non-CAD for both intact and denuded pooled samples.

Preparation of membrane protein

Human adipose arteries/arterioles (200-500 μm) were dissected out from adipose tissues, cleaned off fat and connective tissue, and placed in ice-cold HEPES buffer. Vessel segments were frozen in liquid nitrogen if not used immediately. For some experiments, coronary arteries (200-2,000 μm) were dissected from donor hearts using a similar procedure. Arterial membrane proteins were prepared with a differential centrifugation method as described previously.⁵ All procedures were performed on ice or at 4°C. Briefly, vascular tissues were homogenized with a Tenbroeck glass homogenizer in 2-5 volumes of an ice-cold homogenization buffer (in mmol/L; 20 HEPES pH 7.4, 250 sucrose, 1 EDTA, supplemented with protease and phosphatase inhibitor cocktail), and sonicated at a power setting of 2-3 with a 3-mm microtip at 10 seconds pulses x 3 with 1-2 minute(s) pause on ice (Fisher Scientific Sonci Dismembrator model D100). The homogenates were centrifuged at 3,000 $\times g$ for 10 minutes, the supernatants were transferred to a new tube and centrifuged at 10,000 $\times g$ for 20 minutes, and the supernatants were then centrifuged at 100,000 $\times g$ for 90 minutes (Beckman TLA-100.3 rotor, 50,000 rpm). The pellets containing crude membrane fraction were re-solubilized in a detergent-containing extraction buffer containing (in mmol/L) 25 Tris-HCl pH 7.4, 150 NaCl, 1 EDTA, 1% NP40, 0.5% sodium deoxycholate, and 5% glycerol, supplemented with protease and phosphatase inhibitors. Protein samples were aliquoted, frozen in liquid N_2 , and stored at -80°C until use. Human brain membrane proteins extracted from a normal donor were obtained from BioChain (Newark, CA).

Immunoblotting

Protein samples (20 μg) were separated by SDS-PAGE on 10% gels and transferred to PVDF membranes. Membranes were blocked by 5% NFDM or BSA for 1 hour at room temperature, and incubated overnight at 4°C with one of the following primary antibodies: $K_v\alpha 1.1$ (75-007, NeuroMab K20/48 clone), $K_v\alpha 1.2$ (73-008, NeuroMab K14/16 clone), $K_v\alpha 1.3$ (75-009, NeuroMab L23/27 clone), $K_v\alpha 1.4$ (75-010, NeuroMab K13/31 clone), $K_v\alpha 1.5$ (APC-150, Alomone), $K_v\alpha 1.6$ (75-012, NeuroMab K19/36 clone), BK_{Ca} (75-022, NeuroMab L6/60 clone), and Na^+/K^+ -ATPase (ANP-001, Alomone); 1:2,000 dilution of each antibody in TBST with 5% NFDM or BSA. Blots were then washed with TBST prior to the addition of a HRP-conjugated secondary antibody (1:20,000 dilution in TBST with 5% NFDM or BSA) for 1 hour at room temperature. Membranes were developed using the ECL Prime reagent (Amersham).

Immunohistochemistry

Freshly dissected arteries were embedded in OTC compound, frozen on dry-ice, and cut into 10- μm sections.¹ Some tissue sections were stained with hematoxylin and eosin to confirm the intact vascular structure before further processing for immunofluorescence staining. Tissue sections were washed in PBS and blocked with 5% normal goat serum in PBS containing 0.3% Triton X-100. Sections were then probed with a monoclonal or polyclonal antibody against a specific $K_v1\alpha$ subunit (1:200 dilution) overnight at 4°C, followed by secondary probing with an Alexafluor 568-conjugated goat anti-rabbit or goat anti-mouse IgG antibody for 1 h at room temperature. After several washes with PBS, sections were counterstained with DAPI, a fluorescence nuclear probe, and mounted in SlowFade antifade medium (Invitrogen). Images were immediately captured using a confocal fluorescence microscope (model A1-R, Nikon) with a 60 \times (NA 1.40) oil objective.

Immunocytochemistry

Freshly isolated SMCs, along with sheets of isolated ECs, were allowed to attach to poly-L-lysine-coated 12-mm coverslips for 30 min at 4°C as previously reported.² After several washes with phosphate buffered saline (PBS), cells were fixed with 4% paraformaldehyde for 10 min at room

temperature. Cells were then rinsed 3 times with PBS containing 50 mmol/L NH_4Cl , and blocked with 1% BSA/5% normal goat serum/0.1% saponin in PBS for 30 min. For immunodetection of $\text{K}_\text{V}1\alpha$ subunits, cells were incubated overnight at 4°C with one of the following monoclonal or polyclonal antibodies (1:200 dilution): $\text{K}_\text{V}\alpha 1.3$ (75-009, NeuroMab L23/27 clone), $\text{K}_\text{V}\alpha 1.4$ (75-010, NeuroMab K13/31 clone), $\text{K}_\text{V}\alpha 1.5$ (APC-150, Alomone), $\text{K}_\text{V}\alpha 1.6$ (75-012, NeuroMab K19/36 clone), and BK_Ca (75-022, NeuroMab L6/60 clone). Afterward, cells were rinsed with 1% BSA/0.1% saponin in PBS, followed by incubation for 1 h at room temperature with an appropriate goat secondary antibody conjugated with Alexa Fluor 488 (Invitrogen). The labeled cells were post-fixed with 4% paraformaldehyde for 10 min, and counterstained with the nuclear dye DAPI (300 nmol/L) for 5 min. After several washes with PBS, cells were mounted in SlowFade antifade medium (Invitrogen) and images immediately captured using a confocal fluorescence microscope (model A1-R, Nikon) with a 100 \times (NA 1.45) oil objective.

To confirm the specificity of $\text{K}_\text{V}\alpha 1.5$ antibodies, HEK293 cells transiently expressing h $\text{K}_\text{V}1.5$ -DDK fusion protein and non-transfected HEK293 cells were incubated with rabbit anti- $\text{K}_\text{V}\alpha 1.5$ (1:200 dilution; APC-150, Alomone) and mouse anti-DDK/FLAG (1:500 dilution; TA50011-100, Origene 4C5 clone) followed by Alexa 488-labeled goat anti-rabbit and Alexa 561-labeled goat anti-mouse secondary antibodies, using an immunostaining procedure similar as described above for freshly isolated vascular cells.

Fluorescence data were analyzed using ImageJ (version 1.45s), a public domain program developed at the NIH. Background fluorescence taken just outside of the cells was first subtracted from each image. The fluorescence intensities of eight rectangular user-defined regions of interest (ROIs) both over the plasma membrane (5 x 30 pixels) and in adjacent cytoplasmic areas (5 x 30 pixels) in each cell were measured and averaged to calculate the ratio of plasma membrane to cytoplasmic intensity. Only those ROIs that are free of artifactual staining were included in the analysis. For the analysis of $\text{K}_\text{V}1.5$ and BK_Ca protein localization, the fluorescence ratio was calculated from 6-10 cells each from non-CAD ($n=5$ and 3 for $\text{K}_\text{V}1.5$ and BK_Ca , respectively) and CAD ($n=5$ and 3 for $\text{K}_\text{V}1.5$ and BK_Ca , respectively) subjects. Cells were freshly dissociated from 5-6 pooled segments of arterioles from each subject. The measurement of this ratio is a commonly used method to assess membrane accumulation of protein molecules in cells^{6, 7} and also has been used in our previous studies.²

$\text{K}_\text{V}1.5$ siRNA transfection with reversible permeabilization

Human arteries/arterioles (200-500 μm) freshly dissected from each non-CAD subject were divided into two groups for transfection with control siRNA (ON-TARGETplus non-targeting control pool, D-001810-10-05, GE/Dharmacon) or siRNA against $\text{K}_\text{V}1.5$ (ON-TARGETplus KCNA5 siRNA smart pool, L-006215-00-0005, GE/Dharmacon). Transfection of smooth muscle with control siRNA or $\text{K}_\text{V}1.5$ -specific siRNA were performed using a reversible permeabilization method as previously described.⁸ In brief, arterial segments were sequentially incubated in the following solutions using a 6-well plate with gentle rocking: 1) 20 min at 4°C in Solution I (in mmol/L; 10 EGTA, 120 KCl, 5 ATP, 2 MgCl_2 , 20 TES, pH 6.8 at 4°C); 2) 3 h at 4°C in Solution II (in mmol/L; 120 KCl, 5 ATP, 2 MgCl_2 , 20 TES, pH 6.8 at 4°C) containing 100 nmol/L siRNA; 3) 30 min at 4°C in Solution III (in mmol/L; 120 KCl, 5 ATP, 10 MgCl_2 , 20 TES, pH 6.8 at 4°C) containing 100 nmol/L siRNA. To reverse permeabilization, arterioles were then incubated for 15 min at room temperature in Solution IV (in mmol/L; 140 NaCl, 5 KCl, 10 MgCl_2 , 5.6 glucose, 2 MOPS, pH 7.1, 22°C) containing 100 nmol/L siRNA. After which, the Ca^{2+} concentration of Solution IV was gradually increased from nominally Ca^{2+} -free to 0.01, 0.1, and 1.6 mmol/L every 15 min. Using sterile technique, arterioles were then transferred to DMEM/F-12 (1:1 mixture) culture medium supplemented with 1 mmol/L L-glutamine, 50 U/mL penicillin, and 50 $\mu\text{g}/\text{mL}$ streptomycin, and incubated for additional 24-48 hours in a cell culture incubator (at 30°C in 95% air, 5% CO_2). Arterial samples were assessed for $\text{K}_\text{V}1.5$ mRNA and protein knockdown using RT-

PCR and immunofluorescence as described above. Separated arterial segments were examined for DPO-sensitive and H₂O₂-induced vasodilator response.

Patch-Clamp Recording of K⁺ Currents

Whole-cell K⁺ currents were measured in freshly dissociated smooth muscle cells using the standard (ruptured-patch) or perforated patch-clamp method as previously described.^{9, 10} Patch-clamp was performed with an Axopatch 200B amplifier and pClamp 10 software (Molecular Devices). Patch pipettes were fabricated from borosilicate glass capillaries (glass type 7052) and fire-polished to produce 2 to 4 MΩ tip resistance. Outward K⁺ currents were elicited by progressive 10-mV depolarizing voltage steps (300-ms duration, 5-s intervals) from a holding potential of -70 mV to potentials ranged between -70 and +60 mV. In some experiments, cells were held at -70 mV and linear voltage ramps from -100 to +100 mV (300-ms duration) were applied at a frequency of 0.2 Hz. Currents were filtered at 1 kHz and sampled at 5 kHz. Total cell capacitance and series resistance were estimated by integrating the uncompensated capacitive transients generated by a 10-mV step pulse, and by adjusting the amplifier whole-cell capacitance and series resistance controls to eliminate the resulting current transitions. Series resistance in ruptured whole-cell recordings was <8 MΩ and was not corrected. Amplitude of currents in this configuration was always <1000 pA, resulting in a voltage error of <8 mV. Series resistance in perforated-patch recording was <20 MΩ, and was compensated when currents were >400 pA. All data were corrected for a 10-mV liquid junction potential after the experiment. For each experimental condition in a cell, at least 3 trials were performed and currents were then averaged during analysis. To account for differences in cell membrane surface area, current densities (pA/pF) were calculated by normalization of average whole-cell current to cell capacitance.

The bath solution was composed of (in mmol/L) 140 NaCl, 5 KCl, 0.1 CaCl₂, 1 MgCl₂, 5 glucose, and 10 HEPES (pH 7.4 with NaOH). The pipette solution contained (in mmol/L) 90 potassium aspartate, 30 KCl, 20 NaCl, 1 MgCl₂, 1 Mg-ATP, 1 EGTA, and 10 HEPES (pH 7.2 with KOH). The concentration of free Ca²⁺ in the pipette solution is estimated to be around 10 nM. Contaminating currents through large-conductance, Ca²⁺-activated K⁺ channels (BK_{Ca}) were minimized by lowering free Ca²⁺ concentrations in the pipette and bath solutions, and by including the BK_{Ca} channel blocker paxilline (100 nmol/L) in the bath solution. Perforated patches were used in some experiments by backfilling amphotericin B (100-150 μg/ml in the pipette solution) up to 500-μm distance from the tip of the pipette. Currents were recorded first under control conditions and then after bath perfusion of the drug of interest at the indicated final concentrations. All chemicals were applied to the bath solution by a gravity perfusion system at a flow rate of 1 ml/min. Experiments were performed at room temperature.

Chemicals

DPO-1, paxilline, and Psora-4 were obtained from Tocris, stromatoxin from Alomone, and TCEP from Thermo Scientific. All other chemicals were purchased from Sigma. Stock solutions were made in distilled water, except for the following: CP339818, DPO-1, PAP-1, paxilline, and Psora-4 (ethanol); 4-AP (HCl, pH readjusted to 7.4); and indomethacin (0.1 mol/L Na₂CO₃).

Statistical Analysis

All data are presented as mean±SEM. Comparisons of concentration-response curves of isolated vessels were performed using 2-way repeated measures ANOVA, followed by the Student-Newman-Keuls multiple-comparison test. Other comparisons were made using 1-way ANOVA or Student *t*-test. *P* values <0.05 were considered statistically significant.

For analysis of selected vasodilator responses (e.g., H₂O₂-induced dilation in non-CAD versus CAD group), individual concentration-response curves were fitted to the following 4-parameter sigmoidal logistic equation: $Y_i = P1_i + P2/(1 + \exp(P3 * (\log(X_i) - P4))) + e_i$, where Y_i = vasodilator response, X_i = molar concentration of vasodilator, $P1_i$ = lower plateau response subject random

effect $\{\text{Normal}(\mu_{P1}, \sigma_{P1}^2)\}$, $P2$ = difference between the lower and the maximal plateau responses, $P3$ = slope of concentration-response curve, $P4$ = logarithm of the molar concentration of vasodilator required to produce 50% of the maximal response ($\log EC_{50}$), and e_i = independent error $\{\text{Normal}(0, \sigma_e^2)\}$.¹¹ EC_{50} values were calculated as $-\log EC_{50}$. Nonlinear regression analysis with mixed effects were performed to assess whether coronary artery disease (CAD), risk factors for CAD, age, or gender influenced EC_{50} . Statistical analyses were performed with SAS version 9.4 (SAS Institute Inc., Cary, NC, USA). All other analyses were conducted using the statistical programs in SigmaPlot, version 12.

Supplemental Results

Online Figure I. H₂O₂-induced dilation of non-CAD human adipose arterioles. A, Effect of BK_{Ca} blockade alone and in combination with K_V blockade on H₂O₂-induced dilation. BK_{Ca} channel blocker iberiotoxin (IbTX; 100 nmol/L) also reduced the dilation, and the combination of IbTX and 4-AP (10 mmol/L), a K_V channel blocker, markedly diminished the dilation except for the highest dose of H₂O₂ (100 μ mol/L). $n=6-7$ vessels/group. * $P<0.05$ versus control, # $P<0.05$ versus IbTX. B, Effect of 4-AP on H₂O₂-induced dilation of arterioles. Over-constriction of arterioles (70% \pm 3% from baseline) by 4-AP plus a higher concentration of ET-1 did not further enhance the inhibitory effect of 4-AP on H₂O₂-induced dilation ($n=5$, * $P<0.05$ versus control). C, H₂O₂-induced concentration-dependent dilation in non-CAD arterioles was fitted with a 4-parameter sigmoidal equation. EC_{50} of H₂O₂ was then calculated from the fitted curve. $n=18$ vessels. D, In non-CAD arterioles, selective K_V2.1 and K_V2.1/9.3 blocker stromatoxin (100 nmol/L) did not affect H₂O₂-induced dilation. $n=4$ vessels/group.

Online Figure II. Effects of catalase and thiol-reducing agents on H₂O₂-induced dilation in non-CAD human adipose arterioles. A, The dilation was abolished by H₂O₂ metabolizing enzyme catalase (1000 U/mL) in both intact and denuded vessels. B, The dilation was completely reversed by DTT (3 mmol/L), a membrane-permeable thiol-specific reducing agent, but not by TCEP (5 mmol/L), a membrane-impermeable thiol-reducing agent. DTT had no effect on the dilation induced by papaverine (Pap; 100 μ mol/L), which was added after H₂O₂. * $P<0.05$ versus control (A) or 100 μ mol/L H₂O₂ (B); $n=3-5$ vessels/group.

Online Figure III. Effects of K_V1.5 siRNA on H₂O₂-induced dilation in non-CAD human adipose arterioles. A, H₂O₂-induced dilation was significantly reduced in arterioles treated with K_V1.5 siRNA (% dilation at 10 μ mol/L H₂O₂, 3 \pm 3 vs. 28 \pm 5 with control siRNA, % dilation at 50 μ mol/L H₂O₂, 18 \pm 8 vs. 63 \pm 5 with control siRNA, and % dilation at 100 μ mol/L H₂O₂, 53 \pm 5 vs. 83 \pm 4 in control-siRNA, $n=4$ vessels/group, * $P<0.05$). B, In arterioles treated with control siRNA, the selective K_V1.5 blocker DPO-1 significantly reduced the dilation confirming K_V1.5 channels were functional in these vessels (% dilation at 10 μ mol/L H₂O₂, 12 \pm 4 vs. 28 \pm 5 with control siRNA, % dilation at 50 μ mol/L H₂O₂, 31 \pm 2 vs. 63 \pm 5 with control siRNA, and % dilation at 100 μ mol/L H₂O₂, 62 \pm 6 vs. 83 \pm 4 in control siRNA, $n=4$ vessels/group, * $P<0.05$). C, In contrast, the selective K_V1.5 blocker DPO-1 did not affect the dilation in K_V1.5 siRNA-treated arterioles. $n=4$ vessels/group. D, Three representative gel images of end-point RT-PCR analysis of K_V1.5 gene knockdown (left). Summarized quantitative RT-PCR data (right) indicate that K_V1.5 mRNA expression (normalized to average of β -actin and ATP5o genes) was significantly reduced in K_V1.5 siRNA-treated vessels ($n=4$ vessels/group, * $P<0.05$). Input RNA (cDNA), 20 pg for end-point PCR (left) and 2 ng for quantitative PCR (right), respectively.

Online Figure IV. Immunofluorescence detection of BK_{Ca} and K_V1.5 α -subunits in vascular cells freshly dissociated from human adipose arterioles. A, Expression of BK_{Ca} channel-forming α -subunits (green) in freshly dissociated smooth muscle cells (SMCs) and a sheet of endothelial cells (ECs) from non-CAD and CAD human adipose arterioles. Left, SMCs; right, ECs. B, Expression of K_V1.5 channel-forming α -subunits (green) in freshly dissociated endothelial cells (ECs) from non-CAD and CAD human adipose arterioles. For panels A and B, cell nuclei was stained with DAPI (blue). Scale bar, 10 μ m. Data are representative of >3 independent tissues.

Online Figure V. Immunostaining with K_V1.5 and DDK antibodies. HEK293 cells transiently expressing K_V1.5-DDK (top) and non-transfected cells (lower) were immunolabeled with rabbit polyclonal anti-K_V1.5 antibodies (green) and mouse monoclonal anti-DDK antibodies (red). Cell nuclei was stained with DAPI (blue). Scale bar represents 10 μ m.

Online Figure VI. 4-AP-sensitive voltage-gated K⁺ currents recorded in smooth muscle cells freshly isolated from human adipose arterioles. A, Representative whole-cell currents recorded before (control) and after development of stable inhibition by 5 mmol/L 4-AP, a K_V channel blocker. Currents were elicited by progressive 10 mV depolarizing steps from a holding potential of -70 mV to +60 mV. Cell capacitance was 28 pF. B, Averaged I-V relationships for end-pulse K⁺ currents (normalized to cell capacitance) before and after 5 mmol/L 4-AP ($n=5$ cells each). * $P<0.05$ versus control. C, Concentration-dependent effect of 4-AP (1-10 mmol/L) on outward currents (average of 5-10 current traces) evoked by a ramp depolarization from -100 to +100 mV using the same cell as in panel A.

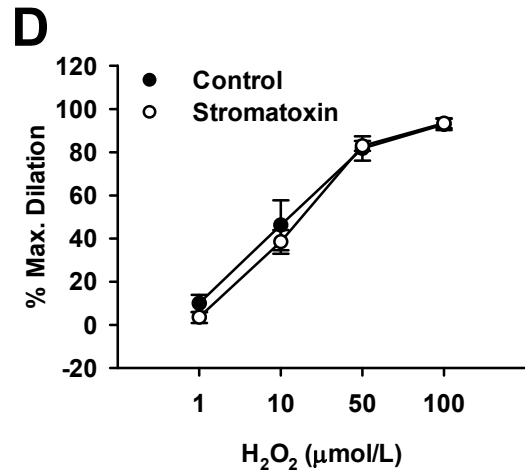
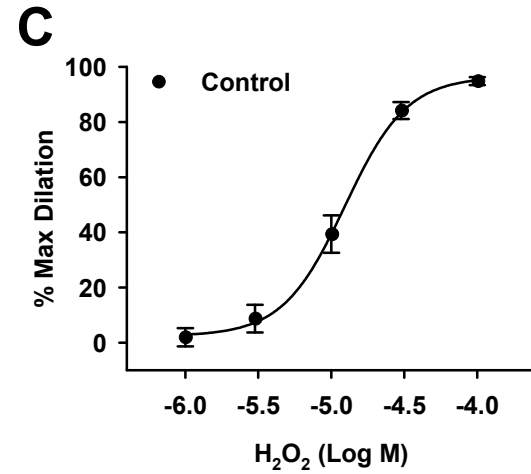
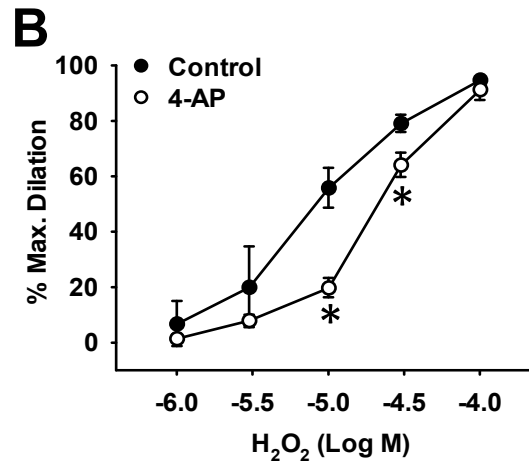
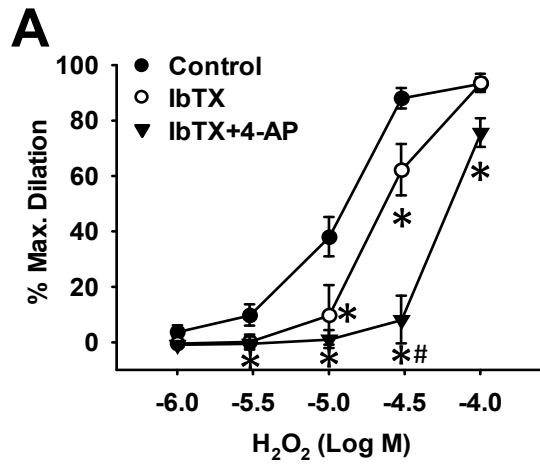
Online Figure VII. Comparison of H₂O₂-induced dilation in adipose arterioles obtained from different regions of the body. There was no significant difference in H₂O₂-induced dilation among visceral, subcutaneous, or pericardial adipose arterioles within non-CAD (A) or CAD (B) subject groups ($n=4-11$ vessels/group).

Online Figure VIII. Interaction of coronary artery disease (CAD) with body mass index (BMI) in influencing EC₅₀ values of H₂O₂ concentration-response curves. H₂O₂ (1-100 μ mol/L)-induced vasodilation were examined in isolated adipose arterioles from non-CAD and CAD subjects. Individual concentration-response curves were statistically fitted to a 4-parameter sigmoidal logistic equation and modeled by non-linear regression analysis with mixed effects to assess the influence of CAD, risk factors for CAD (e.g., BMI), or their interactions on EC₅₀. Plotted EC₅₀ (Log M) data represent fitted values \pm 95% confidence intervals (CI).

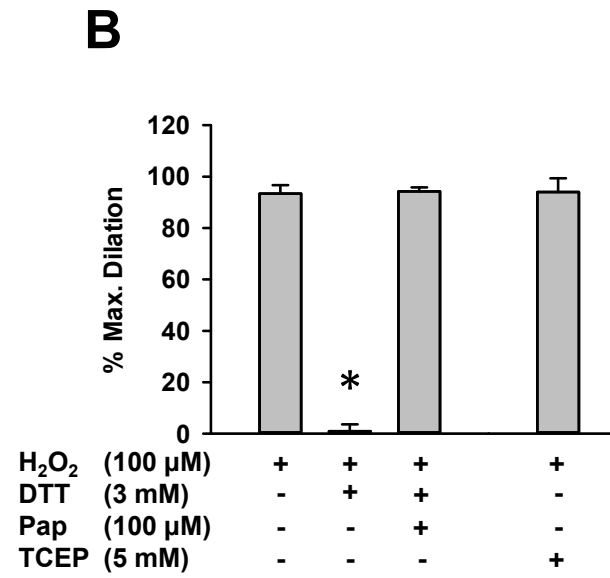
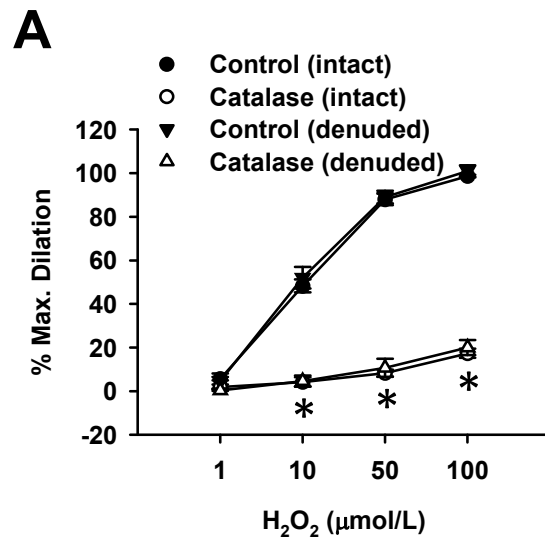
References

1. Mendoza SA, Fang J, Gutterman DD, Wilcox DA, Bubolz AH, Li R, Suzuki M, Zhang DX. Trpv4-mediated endothelial ca^{2+} influx and vasodilation in response to shear stress. *Am J Physiol Heart Circ Physiol*. 2010;298:H466-476
2. Zhang DX, Borbouse L, Gebremedhin D, Mendoza SA, Zinkevich NS, Li R, Gutterman DD. H₂O₂-induced dilation in human coronary arterioles: Role of protein kinase g dimerization and large-conductance ca^{2+} -activated k^{+} channel activation. *Circ Res*. 2012;110:471-480
3. Vacher H, Mohapatra DP, Trimmer JS. Localization and targeting of voltage-dependent ion channels in mammalian central neurons. *Physiol Rev*. 2008;88:1407-1447
4. Kopf PG, Gauthier KM, Zhang DX, Falck JR, Campbell WB. Angiotensin ii regulates adrenal vascular tone through zona glomerulosa cell-derived eets and dhets. *Hypertension*. 2011;57:323-329
5. Zhang DX, Fryer RM, Hsu AK, Zou AP, Gross GJ, Campbell WB, Li PL. Production and metabolism of ceramide in normal and ischemic-reperfused myocardium of rats. *Basic Res Cardiol*. 2001;96:267-274
6. Khalil RA, Morgan KG. Imaging of protein kinase c distribution and translocation in living vascular smooth muscle cells. *Circ Res*. 1991;69:1626-1631
7. Nalaskowski MM, Fliegert R, Ernst O, Brehm MA, Fanick W, Windhorst S, Lin H, Giehler S, Hein J, Lin YN, Mayr GW. Human inositol 1,4,5-trisphosphate 3-kinase isoform b (ip3kb) is a nucleocytoplasmic shuttling protein specifically enriched at cortical actin filaments and at invaginations of the nuclear envelope. *J Biol Chem*. 2011;286:4500-4510
8. Lesh RE, Somlyo AP, Owens GK, Somlyo AV. Reversible permeabilization. A novel technique for the intracellular introduction of antisense oligodeoxynucleotides into intact smooth muscle. *Circ Res*. 1995;77:220-230
9. Gollasch M, Ried C, Bychkov R, Luft FC, Haller H. K^{+} currents in human coronary artery vascular smooth muscle cells. *Circ Res*. 1996;78:676-688
10. Zhang DX, Gauthier KM, Chawengsub Y, Campbell WB. Ach-induced relaxations of rabbit small mesenteric arteries: Role of arachidonic acid metabolites and k^{+} . *Am J Physiol Heart Circ Physiol*. 2007;293:H152-159
11. Stork AP, Cocks TM. Pharmacological reactivity of human epicardial coronary arteries: Characterization of relaxation responses to endothelium-derived relaxing factor. *Br J Pharmacol*. 1994;113:1099-1104

Online Figure I

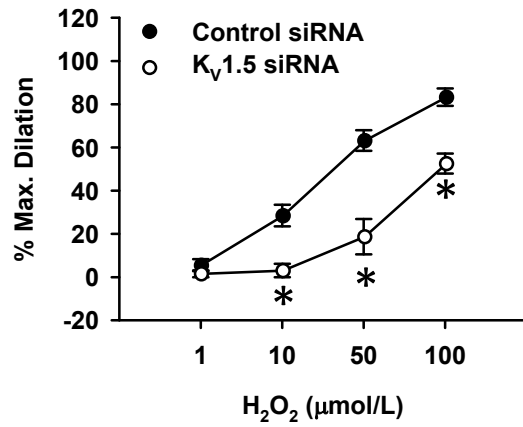


Online Figure II

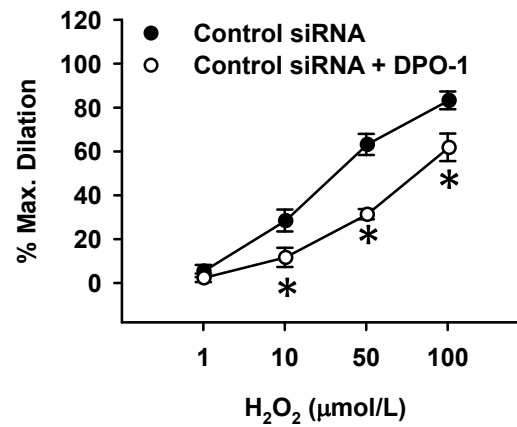


Online Figure III

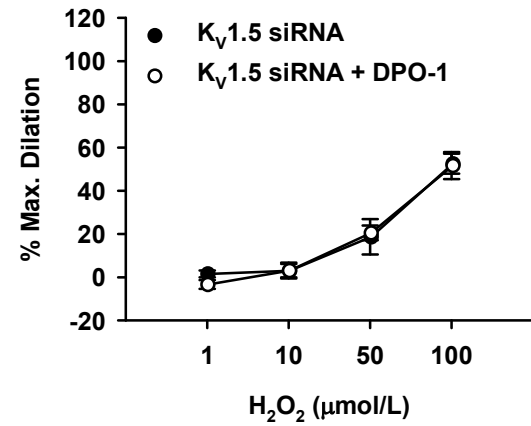
A



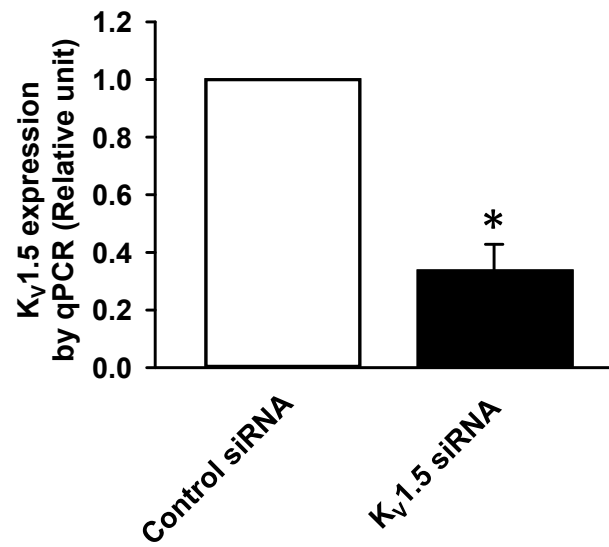
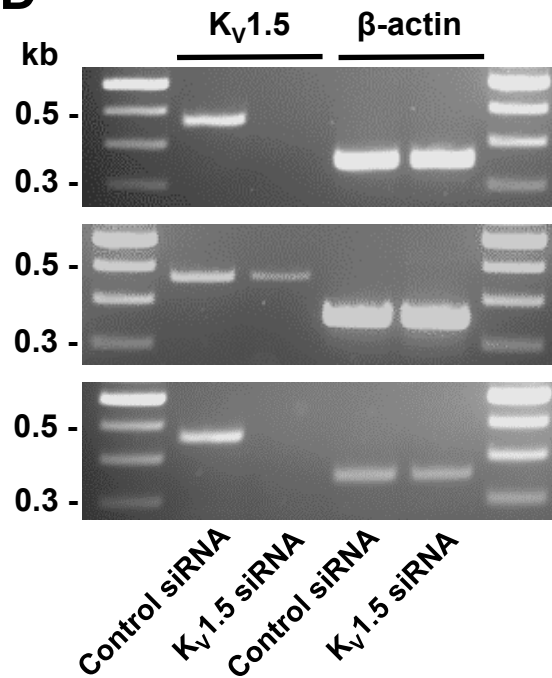
B



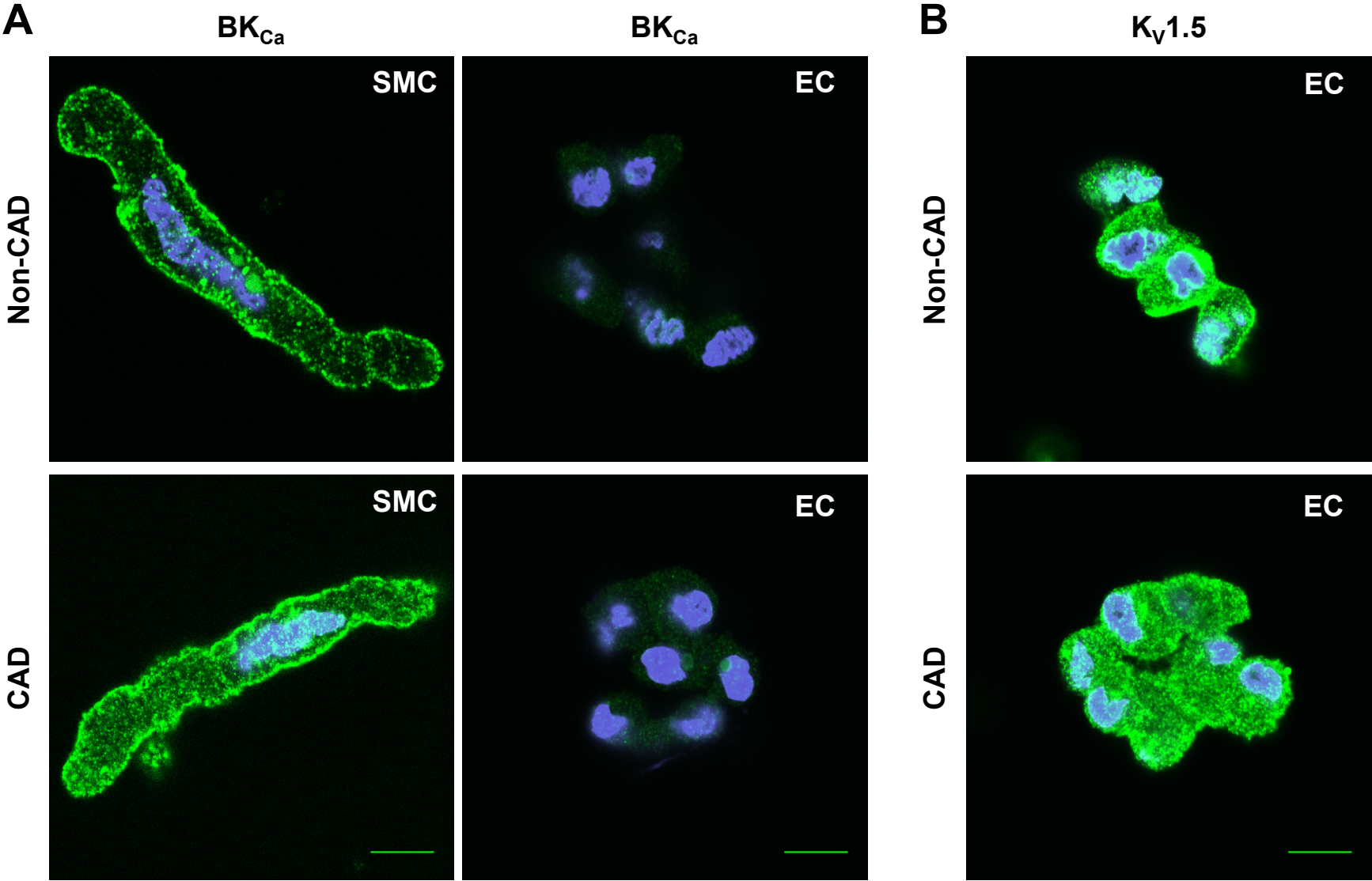
C



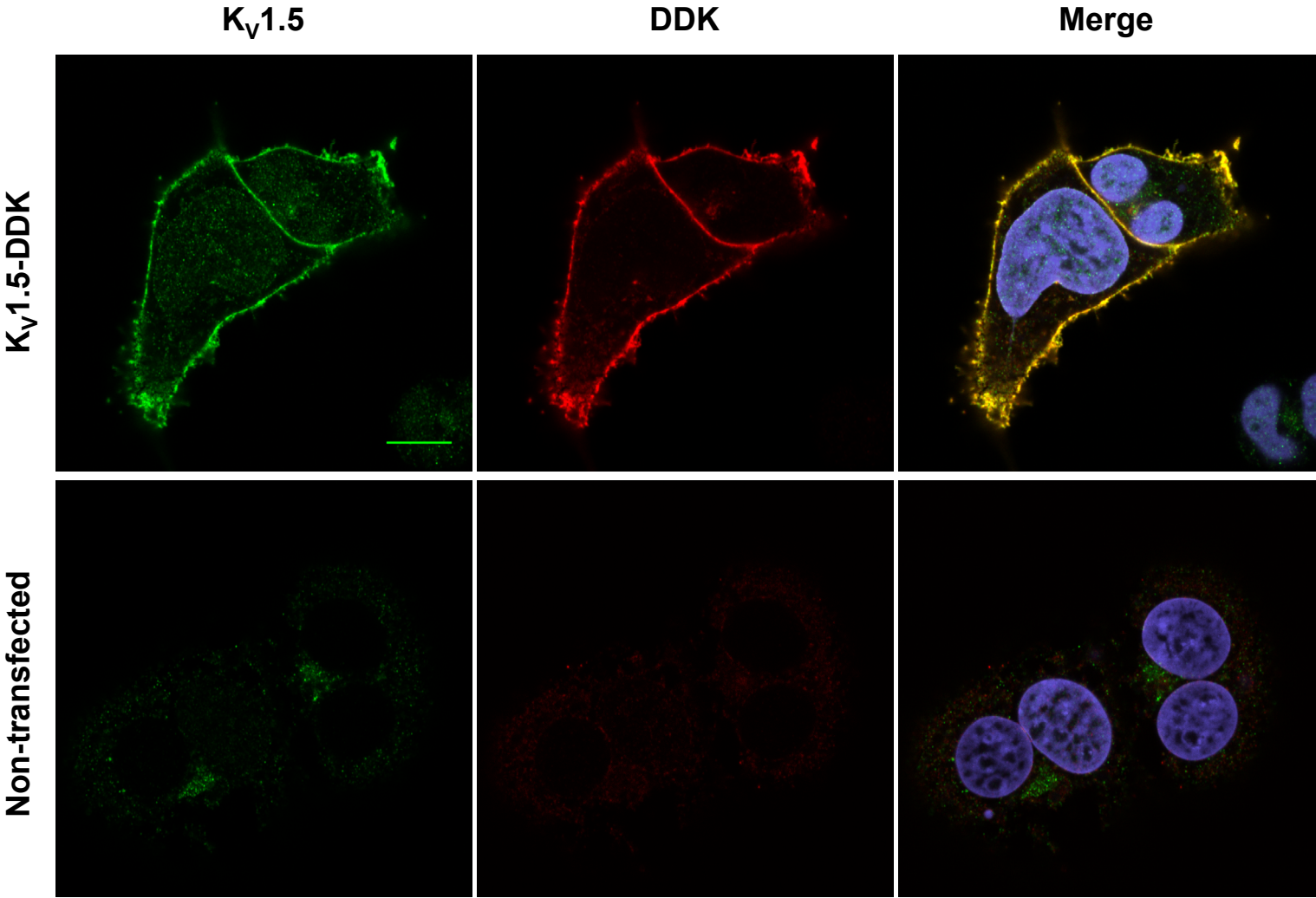
D



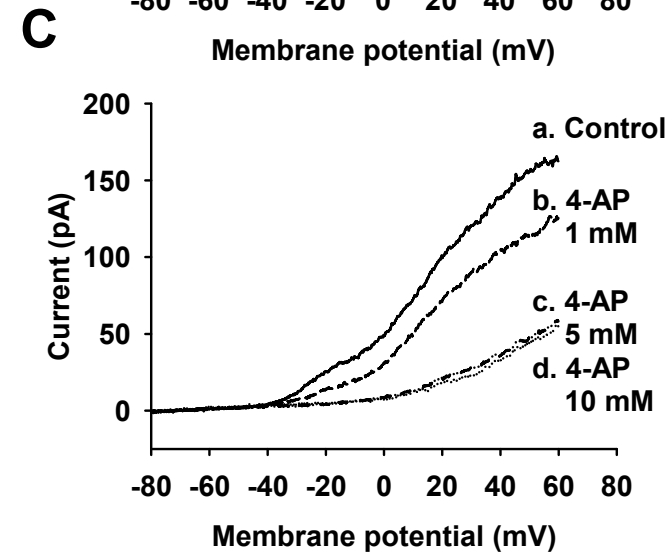
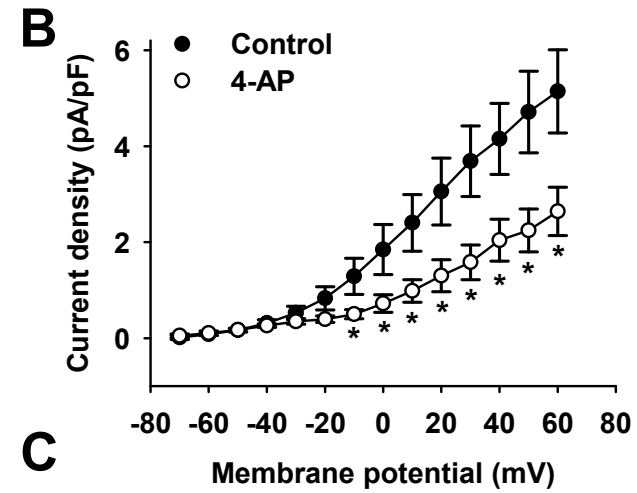
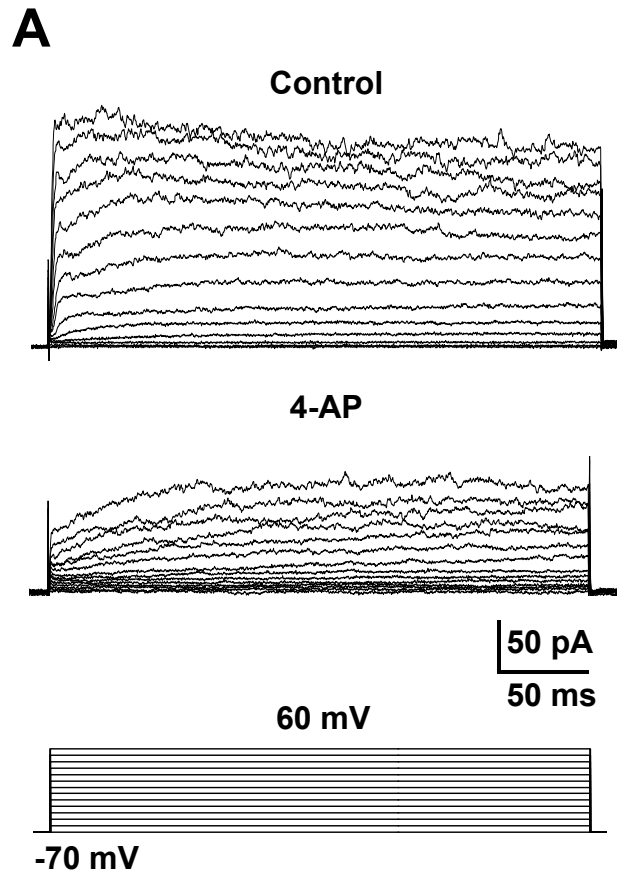
Online Figure IV



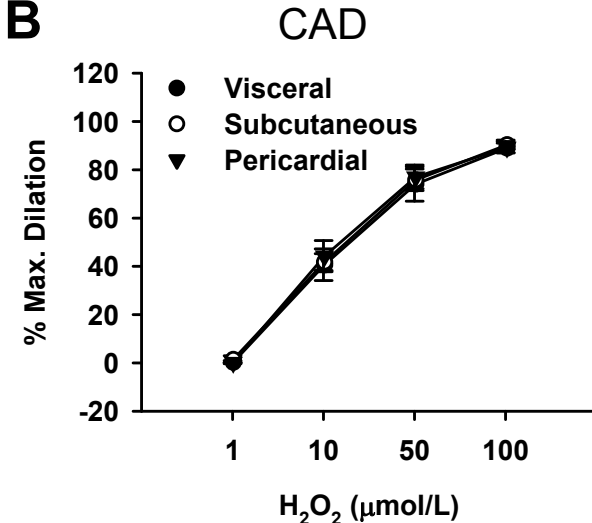
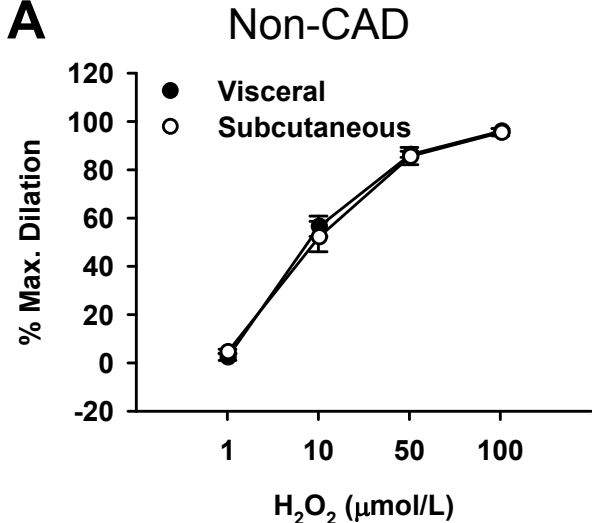
Online Figure V



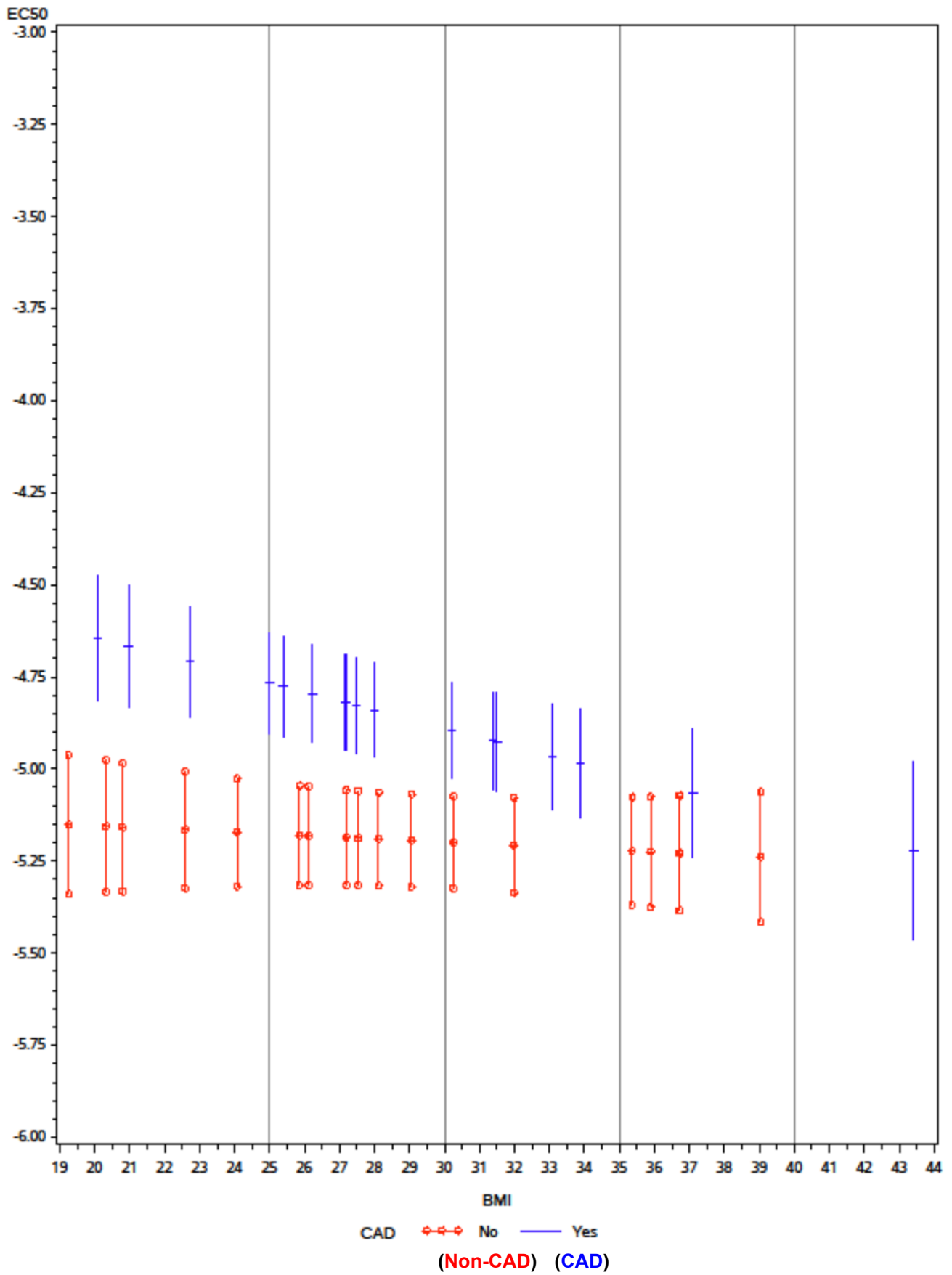
Online Figure VI



Online Figure VII



Online Figure VIII



Online Table I.

Patient demographics ($n=134$)

	Adipose ($n=120$)		Donor heart ($n=14$)	
	non-CAD ($n=79^*$)	CAD ($n=41^{\dagger}$)	non-CAD ($n=7$)	CAD ($n=7$)
Gender, Male/Female	22(28%)/57(72%)	31(76%)/10(24%)	3(21%)/4(79%)	7(100%)/0
Age, yr (mean \pm SEM)	49 \pm 16	66 \pm 9	43 \pm 14	59 \pm 8
Body mass index (mean \pm SEM)	30 \pm 7 \ddagger	30 \pm 7	28 \pm 7	32 \pm 7
Underlying diseases/Risk factors				
Coronary artery disease	0	41(100%)	0	7(100%)
Hypertension	15(19%)	21(51%)	2(29%)	5(71%)
Hyperlipidemia	8(10%)	17(42%)	0	3(43%)
Diabetes mellitus	4(5%)	10(24%)	0	0
Atrial fibrillation	0	4(10%)	0	1(14%)
Congestive heart failure	0	3(7%)	0	0
Myocardial infarction	0	5(12%)	0	2(29%)
(Tobacco use)	6(8%)	9(22%)	2(29%)	3(43%)
None of the above	45(57%)	11(27%)	4(57%)	0

$*$, pericardial $n=2$, visceral $n=52$, subcutaneous $n=25$

\dagger , pericardial $n=22$, visceral $n=16$, subcutaneous $n=3$

\ddagger , Total of 2 patients with no information on height and weight.

Online Table II

Characteristics of isolated adipose arterioles

	Internal Diameter, μm			Endothelin-1	Precontraction (%)	Number of arteries
	Passive	Active (without blocker)	Active (with blocker)			
Non CAD						
Control (+L-NAME & Indo)	145 \pm 10	145 \pm 9	144 \pm 10	74 \pm 13	47 \pm 5	5
10 mM 4-AP	159 \pm 13	154 \pm 11	99 \pm 16*	64 \pm 13	54 \pm 7	5
Control (+L-NAME & Indo)	160 \pm 24	147 \pm 25	145 \pm 28	92 \pm 22	38 \pm 6	5
10 mM 4-AP (over-constriction)	160 \pm 24	152 \pm 22	104 \pm 27*	46 \pm 10	70 \pm 3	5
Control (+L-NAME & Indo)	183 \pm 20	180 \pm 20	179 \pm 21	92 \pm 13	49 \pm 7	5
100 nM paxilline	178 \pm 24	174 \pm 24	159 \pm 31	73 \pm 14	50 \pm 6	5
Control (+L-NAME & Indo)	247 \pm 14	229 \pm 25	233 \pm 22	153 \pm 11	38 \pm 2	7
100 nM IbTX	250 \pm 16	242 \pm 15	242 \pm 15	148 \pm 20	41 \pm 5	6
100 nM IbTX + 10 mM 4-AP	247 \pm 14	226 \pm 19	152 \pm 27*	66 \pm 13	75 \pm 4	7
Control (+L-NAME & Indo)	146 \pm 10	143 \pm 9	146 \pm 10	83 \pm 13	43 \pm 4	5
1 μM DPO-1	147 \pm 8	144 \pm 8	117 \pm 18	73 \pm 12	51 \pm 3	5
Control (+L-NAME & Indo)	149 \pm 12	148 \pm 12	146 \pm 11	82 \pm 11	45 \pm 6	5
30 nM Psora-4	148 \pm 12	145 \pm 12	132 \pm 14	88 \pm 8	36 \pm 2	5
Control (+L-NAME & Indo)	150 \pm 13	149 \pm 12	149 \pm 13	87 \pm 9	44 \pm 3	5
10 nM PAP-1	147 \pm 12	142 \pm 14	141 \pm 13	83 \pm 11	45 \pm 3	5
Control (+L-NAME & Indo)	163 \pm 16	162 \pm 13	160 \pm 15	84 \pm 7	47 \pm 2	5
3 μM CP-339818	163 \pm 16	162 \pm 16	157 \pm 14	77 \pm 10	51 \pm 4	5
Control (+L-NAME & Indo)	166 \pm 21	155 \pm 21	157 \pm 20	93 \pm 13	41 \pm 3	4
100 nM stromatoxin	166 \pm 21	152 \pm 21	151 \pm 20	87 \pm 19	48 \pm 6	4
CAD						
Control (+L-NAME & Indo)	165 \pm 28	164 \pm 28	163 \pm 28	85 \pm 17	46 \pm 1	6
10 mM 4-AP	183 \pm 26	181 \pm 26	134 \pm 12	74 \pm 12	50 \pm 4	6
Control (+L-NAME & Indo)	134 \pm 14	133 \pm 14	126 \pm 15	63 \pm 10	47 \pm 4	5
100 nM paxilline	134 \pm 14	131 \pm 12	117 \pm 10	66 \pm 11	49 \pm 5	5
Control (+L-NAME & Indo)	139 \pm 15	137 \pm 13	137 \pm 16	75 \pm 7	47 \pm 3	5
1 μM DPO-1	136 \pm 21	134 \pm 17	127 \pm 19	68 \pm 9	48 \pm 6	5
Control (+L-NAME & Indo)	178 \pm 23	176 \pm 22	173 \pm 23	115 \pm 15	35 \pm 1	3
30 nM Psora-4	177 \pm 22	173 \pm 22	166 \pm 18	113 \pm 18	39 \pm 4	3

Values are means \pm SEM of H₂O₂-induced dilation. Indo, indomethacin; 4-AP, 4-aminopyridine; IbTX, iberiotoxin.

**P* < 0.05 indicates significant difference in active diameters with and without inhibitors as determined using paired t-test.

All experiments shown in this table were performed on endothelium-intact arterioles and in the presence of L-NAME and Indomethacin.

Online Table III.

Nucleotide sequence of Primers used for PCR

For traditional end-point PCR		
Transcript	Forward and Reverse primers	Amplicon size, bp
K _V α1.1	5'-AGT CGC ACT TCT CCA GTA TCC-3' 5'-TCG GTC AGT AGC TTG CTC TTA T-3'	424
K _V α1.2	5'-TCA AGT TGT CCA GAC ACT CCA A-3' 5'-TGT GTT AGC CAA GGT ACA GTT G-3'	548
K _V α1.3	5'-CTT CAG GTT TCA GCA GCA TCC-3' 5'-GCA GGT GGC AGT GGA ATT G-3'	395
K _V α1.4	5'-GAG GCG GAT GAA CCT ACT ACC-3' 5'-CCC TTT CCC TGA CAC TTC TCC-3'	401
K _V α1.5	5'-CCG TCT ACT TCG CAG AGG CT-3' 5'-CCA GGC AGA GGG CAT AAA GG-3'	465
K _V α1.6	5'-AGA GGC TGA CGA TGA CGA TTC-3' 5'-CCG ATG TGG TGT AGG AAG GTA G-3'	364
K _V α2.1	5'-GGC TTG CTC ATC CTC TTC CTT-3' 5'-TCT CCT GTC TCT TCT GCT CCT T-3'	289
K _V α9.3	5'-GGC TTC TGC TTC TCT TCC TCT-3' 5'-ACT GGT CCA CAT CAA TGT CCT T-3'	297
K _V β1.1	5'-CAG CAG CCT TAG TCC CTC AG-3' 5'-GCC GTT CAG CAA CCT CAT CT-3'	239
K _V β1.2	5'-GTG GAG CAG CCG AAC AGA A-3' 5'-GCC GTT CAG CAA CCT CAT CT-3'	192
K _V β1.3	5'-ACC TCT CGT GAC TGC CTG T-3' 5'-GCC GTT CAG CAA CCT CAT CT-3'	378
BK _{Ca} α	5'-ATG CGG AAC TCA CCC AAC A-3' 5'-TCG CCA AAG ATG CAG ACC AC-3'	224
β-actin	5'-GCT CGT CGT CGA CAA CGG CTC-3' 5'-CAA ACA TGA TCT GGG TCA TCT TCT C-3'	353
For quantitative PCR (qPCR)		
Transcript	Forward and Reverse	Amplicon size, bp
K _V α1.5	5'-CGTCATCGTCTCCAACCTTCAAC-3' 5'-TTCCGCTGGACTCCTCTGT-3'	126
ATP synthase O subunit	5'-TCTCCTTTAGAAGAAGCCACACT-3' 5'-GCACAATCATTCCACCCAAGAT-3'	124
β-actin	5'-GCACTCTTCCAGCCTTCCTT-3' 5'-TGTGTTGGCGTACAGGTCTT-3'	114